Atmos. Chem. Phys. Discuss., 10, 27075–27098, 2010
www.atmos-chem-phys-discuss.net/10/27075/2010/
doi:10.5194/acpd-10-27075-2010

Atmospheric Chemistry and Physics Discussions

Spectral albedo of arctic snow during intensive melt period

O. Meinander[1], **S. Kazadzis**[2], **A. Arola**[3], **R. Kivi**[4], **A. Kontu**[4], **H. Suokanerva**[4], **V. Aaltonen**[1], **T. Manninen**[1], **J.-L. Roujean**[5], **and O. Hautecoeur**[5]

[1]Finnish Meteorological Institute, P.O. Box 503, 00101 Helsinki, Finland
[2]Institute for Environmental Research and Sustainable Development, National Observatory of Athens, Greece
[3]Finnish Meteorological Institute, Kuopio Unit, P.O. Box 1627, 70211 Kuopio, Finland
[4]Finnish Meteorological Institute, Arctic Research Centre, Tähteläntie 62, 99600 Sodankylä, Finland
[5]Meteo-France/Centre National de la Recherche Scientifique (CNRS), Toulouse, France

Received: 17 August 2010 – Accepted: 21 October 2010 – Published: 9 November 2010

Correspondence to: O. Meinander (outi.meinander@fmi.fi)

Published by Copernicus Publications on behalf of the European Geosciences Union.

Abstract

Spectral albedo and water liquid content of intensively melting Arctic snow were measured during the Snow Reflectance Transition Experiment (SNORTEX), in Sodankylä, Finland, in April 2009. The upwelling and downwelling spectral irradiance, measured at 290–550 nm with a double monochromator spectroradiometer, revealed the snow albedo to increase as a function wavelength. At the same time, we found the albedo of melting snow to decrease by ∼10%, as a function of time within one day. During four days of intensive snow melt, the albedo decreased from 0.65 to 0.45 at 330 nm, and from 0.72 to 0.53 at 450 nm. The diurnal decrease in albedo was supported by measurements of erythemally weighted broadband ultraviolet (UV) albedo. Our simultaneous ancillary data on snow water liquid content showed that the water content first increased in the surface layer, and then moved into deeper layers, after several hours of accumulation. In Radiative Transfer (RT) model calculations, the use of Lambertian assumed regional albedo, instead of the measured local albedo, showed a wavelength dependent difference between the modeled and the measured radiation by up to 9%.

1 Introduction

The albedo of a surface results from the target's capability to reflect wavelength-dependently the direct and diffuse irradiance. For snow, the albedo is typically very high compared to other natural objects or surfaces. When the albedo of a snow surface at the ground is measured at a standard height of 1–2 m (WMO, 2008, p. I.7–19), it is not only the target's basic properties; like snow age, grain size, water content or dirt; but also the overall environment around the target that may have effect on the detected albedo. Physical, chemical, and biological environmental factors may be included; for example, if the target, or the sensor, are in total or penumbral shadow. Also, topography may affect the measured albedo despite a flat measurement area; chemical reactions may take place in the snow (Grannas et al., 2007); and bacteria may be important for the snow formation (Christner et al., 2008). Finally, the ability of detecting accurately the albedo of a surface depends on the measurement uncertainties and errors introduced by the measuring systems (e.g., Bernhard and Seckmeyer, 1999).

The albedo of snow on the ground can be very variable and inhomogeneous (e.g., Zhou et al., 2003; Kylling et al., 2000). The irradiance ratios are influenced not only by the local snow albedo underneath the measuring radiometers, but also the combination of low-albedo and high-albedo surfaces within a larger radius. Often an effective albedo is defined to describe the net effect of the albedo, as derived by comparison with a model, (Schwander et al., 1999; Kylling et al., 2000; Bernhard et al., 2007, e.g.).

In this work, the main focus was to study the spectral albedo of melting Arctic snow with the help of spectral up-welling and down-welling measurements, combined with various ancillary data, and with the modeling of diffuse and direct spectral irradiance at ultraviolet and visible wavelengths. For the albedo measurements, a Bentham-spectrometer setup with two entrance optics (Sect. 2.2), performed irradiance measurements during the SNORTEX-2009 campaign (Sect. 2.1) in the European Arctic, Northern Finland. For investigating the effect of the changing albedo on the irradiance measured at the ground, we used the Libradtran RT model calculations (Mayer and Kylling, 2005), with additional measurements as model input.

2 Materials and methods

2.1 The SNORTEX experiment

SNORTEX (2008–2010) aims at acquiring in situ measurements of snow and forest properties in support to the development of modeling tools, and to validate coarse resolution satellite products (Roujean et al., 2009, 2010). The SNORTEX studied area is located in the Finnish Lapland beyond the Arctic Circle, and benefits from existing facilities provided by the Finnish Meteorological Institute – Arctic Research Center (FMI-ARC), based in Sodankylä (67°22′ N, 26°39′ E, 179 m a.s.l.). The aim of the project is to integrate its results into operational chains devoted to map snow properties from the MetOp satellite within the framework of the SAF (Satellite Application Facilities) Land, Climate and Hydrology activities, supported by EUMETSAT and the National Meteorological Services.

2.2 Bentham spectrometer

The Bentham spectroradiometer participated in the SNORTEX-2009 campaign (April period) at Sodankylä. The instrument operated from 20 to 25 April, performing down-welling and up-welling spectral measurements of global irradiance (irradiance received by a flat sensor surface), at the 290–550 nm wavelength range at 2.5 m height. These measurements were used to retrieve spectral albedo of the snow surface. The Bentham spectroradiometer consists of a commercially available Bentham DM-150 double monochromator with a focal length of 150 mm monochromator, and with gratings of 2400 lines/mm. The entrance and exit slit widths were chosen to yield a nearly triangular slit function, with a full width at half maximum (FWHM) resolution of 0.74 nm. The solar irradiance is sampled through a specially designed entrance optics (CMS-Schreder, Model UV-J1002), connected to the port of the spectroradiometer through a quartz fiber. The fiber optic splits and leads to two identical entrance optics receivers (diffusers) that can be distinguished through an internal switch. The angular response of the two diffusers is better than 2% for incident angles less than 70 degrees. As the instrument is designed for outdoor solar measurements, the whole spectroradiometer system, including the data-acquisition electronics, is contained in a temperature-controlled box that is stabilized to a predetermined temperature with a precision of 0.5 K. Absolute irradiance scale calibration is performed using measurements of calibrated 1000 W quartz halogen lamps. To measure at locations far from its laboratory, a portable irradiance scale was devised. It is composed of a portable lamp enclosure (calibrator), a set of 100 and 250 W tungsten halogen lamps, and a feedback system. For the particular campaign, the two entrance optics were used for measurements of the down-welling and the up-welling global solar irradiance. The calibration of the

Discussion Paper | Discussion Paper | Discussion Paper | Discussion Paper |

ACPD

10, 27075–27098, 2010

Spectral albedo of arctic snow during intensive melt period

O. Meinander et al.

instrument was performed at the beginning, and at the end of the campaign, showing deviations within 1% for all spectral range, and all three lamps used for the calibration procedure.

2.3 Ancillary measurements

Ancillary albedo data were provided by two broadband radiometers (Model SL501, Solar Light Co.), above another field at ~20 m distance. These continuous SL501 snow albedo measurements were started in 2007, as part of the International Polar Year IPY (2007–2008) ORACLE-O3 cluster project (Ozone layer and UV radiation in a changing climate evaluated during IPY, http://www.awi-potsdam.de/atmo/ORACLE-O3) (Meinander et al., 2008, 2009). Two well maintained and calibrated SL501 sensors with similar spectral and cosine responses were used; one facing upwards, and the other downwards, at a height of 2 m. The data are recorded in 1-min intervals and stored in the FMI climate database. The SL501 spectral response approximates the action spectrum for erythema at the wavelengths of UVB (280–310 nm) (Seckmeyer et al., 2005). The albedo of snow was calculated from the ratio of up-welling UV irradiance to downwelling irradiance.

For the measurement of snow water liquid content, we used the Snow Fork by Toikka Oy (www.toikkaoy.com). The sensor is a steel fork that is used as a microwave resonator. Snow Fork measures the electrical parameters: resonant frequency, attenuation, and 3-dB bandwidth used to calculate accurately the complex dielectric constant of snow. Furthermore, the liquid water content and density of snow are calculated using semi-empirical equations.

We measured the snow grain size and temperature of the snow surface at various depths for the same snow field as the spectral albedo. The measurements were performed at the edge of this field to cause a minimum disturbance for the radiation measurements. The grain sizes of snow were estimated visually with a mm-grid. The snow temperature was measured with a light digital Printel thermometer (www.printel.fi). The thermometer was calibrated using isopropanol measured with a Fluke accuracy

ACPD
10, 27075–27098, 2010

thermometer in the measured temperatures from −20.72 °C to +1.218 °C at 99 different temperatures. Empirical calibration was calculated and the measured snow temperatures were corrected using this calibration. In addition, data on the state of the atmosphere, at a height of 2 m, were being measured once a minute by an automatic weather station (AWS).

2.4 RT model calculations

We used the Libradtran RT model (Mayer and Kylling, 2005) to calculate the up-welling and down-welling diffuse and direct spectral irradiances during a cloudless sky day (22 April). The measured spectral albedo (Bentham spectroradiometer data), total ozone (Sodankylä ozone sounding data, http://fmiarc.fmi.fi/archive/), and aerosol properties measured with a Precision Filter Radiometer/SunPhotometer (http://litdb.fmi.fi/), were used as main inputs for the RT calculations. Our research question was: How much does the modeled clear sky irradiance (if assuming regional Lambertian albedo, or if using the local measured albedo) differ as a function of time and wavelength from the measured irradiance. A difference in irradiance in [%], in the morning and afterwards, would indicate about radiative forcing differences due to the effect of albedo of melting snow. In addition, in model to measured comparison, only relative changes [%] in irradiances were compared, instead of absolute values, to eliminate the effect of absolute calibration scale uncertainties of the measurement data. Absolute calibration scale should not affect the albedo measured by the Bentham spectroradiometer, as the same monochromator/light directing system is used for both the upward and downward sensors. The estimates for the regional albedo values were gained from the measured albedo minimum (A_{min}) and maximum (A_{max}).

ACPD
10, 27075–27098, 2010

3 Results

For the analysis of the empirical data and the RT model data, we used data for solar zenith angle (SZA) < 70° (06:00 UTC – 14:00 UTC). The amount of radiation reaching the Earth is minimal at larger SZA, (UVI < 1), increasing the uncertainties in the measurements.

3.1 Spectral albedo changes

The surface underneath the two Bentham sensors, at the height of 2.5 m from the ground, was covered with snow in a radius of more than 10 m on the South, West and East direction, and up to 3 m in the North direction. The field of view of the sensors was mostly free. Direct Sun irradiance was blocked by trees from 03:00 to 05:00 UTC, and after 17:00 UCT. In addition, shadows of the trees were covering all or part of the snow surface underneath the instruments in the morning till 06:10 UTC, and after 15:30 UTC. The measurement sequence included simultaneous spectral scans of down-welling and up-welling global irradiance (290–550 nm with a wavelength step of 10 nm), with a time step of 2 to 6 min. The different time step was used in order to avoid uncertainties in the albedo calculations that could be inherited by the radiation field changes between the two measurements. For clear sky conditions the 6 min time step, and for moving clouds conditions the 2 min step were used. For 21 and 23 April, the sky conditions were cloudy with moving clouds, resulting changes in the radiation field (Fig. 1). The 22 April consisted of a cloudless day, and 24 April an overcast day with mainly diffuse sky conditions.

During these four days, high temperature conditions lead to intensive melt procedures. The albedo at 330 nm decreased from ~0.65 (the morning of the first day) to 0.45 (the afternoon of the fourth day). At 450 nm, the decrease was from 0.72 to 0.53, accordingly. During one day, the albedo decreased by appr. 10%. In the mornings, the albedo signal was slightly higher than it had been the previous evening, possibly due to frost conditions during the night time (Fig. 2).

ACPD
10, 27075–27098, 2010

We calculated the SZA dependent empirical albedo decline, using a simple linear regression approach (albedo = f·SZA). For our case, the parametrization of albedo of melting snow during the clear sky day was:

$$A(\lambda, \mathrm{SZA}) = A_{\mathrm{midday}} + c(\mathrm{SZA} - \mathrm{SZA}_{\mathrm{min}}), \tag{1}$$

where $c = -0.0024$ before noon, $c = -0.0026$ after noon, for 310 nm $> \lambda >$ 550 nm, $55 < \mathrm{SZA} < 70$ degrees.

For example, for 22 April, from 06:00 to 10:00 UTC, it was $c = (0.572691 - 0.604647)/(68.9 - 55.38)$.

Independently from the temporal decrease of albedo, the snow albedo at one time increased as a function of wavelength (Fig. 3). During the clear sky day of 22 April, the spectral behavior of snow albedo was analyzed further. An average of ∼8% difference on the calculated albedo was found comparing UVB (at 320 nm) and visible (at 550 nm) wavelengths. Deviations up to 5% from this spectral behavior could be seen during the day. We then calculated the mean values for UV-B (at 310 nm), UV-A (at 330–360 nm) and visible (at 450–550 nm). The regressions of snow albedo A at UV-A, UV-B, and VIS were:

$$A(\text{UV-A}) = 1.0049A(\text{UV-B}) + 0.0054, (R^2 = 0.9744), \tag{2}$$

and

$$A(\mathrm{VIS}) = 1.1602A(\text{UV-B}) - 0.0213, (R^2 = 0.6012), \tag{3}$$

for $\mathrm{SZA} < 70.0$ degrees

3.2 Ancillary measurement results

The diurnal decrease of albedo was supported by the broadband UV albedo measurements, representing another smaller open field close by. This broadband erythemal SL-501 albedo decreased both within a day (from morning till afternoon), and as a

ACPD
10, 27075–27098, 2010

function of time (days). The decrease at the end of April (17–30 April) was from 0.51 to 0.38 in the morning, and from 0.48 to 0.37 in the afternoon (Fig. 4). For example, on 22 April, from 06:00 UTC to 12:00 UTC, the decline was $A = -0.0028 \cdot \mathrm{SZA}$ (SZA changed from 68.9 to 58.13, and albedo from 0.47 to 0.43).

The data on snow water liquid content, as a function of time and snow depth, on the same field as the Bentham measurements, showed that the water content first increased in the surface layer. After several hours of accumulation, the water moved into deeper layers (Fig. 5). The snow temperature of the same area showed both a vertical and temporal increase during the study days (Fig. 6). The snow surface observations indicated the intensive melt on 22 April, with snow grain sizes changing from 0.25 mm up to several millimeters (Table 1). The AWS data showed that at 06:00 UTC the air temperatures were $<0\,^{\circ}$C during 20–21 April, and $>0\,^{\circ}$C on 22–24 April. The maximum air temperatures varied from -2.5 to $5.4\,^{\circ}$C. At 18:00 UTC, the air temperature were $>0\,^{\circ}$C on 20–24 April, with maximum temperatures from 0.5 to $9.5\,^{\circ}$C. Between 20–24 April, the automatically measured snow height declined from 48 cm to 38 cm (data not shown), and in the open field of our spectral albedo measurements it was manually measured to change from 30 cm to partly totally melted.

3.3 RT modeling

For the clear sky day 22 April, the spectroradiometer measured albedo minimum was $A_{\mathrm{min}} = 0.54$, and the maximum $A_{\mathrm{max}} = 0.65$ at 330 nm. These were used as input parameter values for the RT calculations representing the assumed effective Lambertian (L) albedo $A(t,L)$, and further compared with calculations using the actual measured spectral albedo $A(\lambda,t)$ as input. The values of the other measured input parameters for the both types of RT calculations were: Ångström parameters $\alpha = 1.253$ and $\beta = 0.038$ (for the calculation of $\tau_a = \beta\lambda^{-\alpha}$, where α is the Ångström exponent and β is the aerosol optical thickness), and 347 DU for ozone. Thereafter, the irradiance was modeled from 06:00 UTC to 14:00 UTC to produce the spectra S1(t, $A_{\mathrm{min}}(L)$), S2(t, $A_{\mathrm{max}}(L)$), and

ACPD
10, 27075–27098, 2010

S3(t, $A(\lambda)$), where S1 is spectrum number 1, t is time, A is albedo, and L is the Lambertian assumed reflectance. The maximum difference was to appear with A_{max}, as in reality the albedo was decreasing as a function of time. For the same reason, the measured irradiance was expected to be closest to the case of A_{min}, as confirmed by our modeling results (data not shown). The differences were 2.5–4.5% for wavelengths from 320 to 400 for this one day showing the 10% change in the albedo (Fig. 7). The difference was calculated up to 9% when using the results for the 4 days of the melting snow period.

4 Discussion

Our albedo results on the melting Arctic snow showed a rapid decrease in the albedo as a function of time. Here, due to the intensively melting snow, the albedo decline was found to dominate over the SZA dependent albedo signal. Thus, a SZA asymmetric albedo was detected. The same asymmetrical decrease feature has also been found, e.g., by Pirazzini (2004) in the Antarctic at three locations; Pirazzini et al. (2006) in the Arctic snow and ice albedo data; and Meinander et al. (2009) in the Arctic and Antarctic data. According to Pirazzini (2004), the SZA asymmetry of the Antarctic snow was: $A = A_{midday} + c(\text{SZA-SZA}_{min})$, where $c = -0.003$ was the best value for c in the afternoon. Their measurements were made with pyranometers (broadband signal for ~300 nm – 3000 nm). In Meinander et al. (2009), the reported UV albedo decline was $A = -0.0024 \cdot \text{SZA}$ for the same Antarctic location of Neumeyer, same season, and similar weather conditions as in Pirazzini (2004), but for different instrument (SL-501) and wavelength range. Here, we found the Bentham data to show a decline from $A = -0.0024 \cdot \text{SZA}$ to $A = -0.0026 \cdot \text{SZA}$ in a big open field with intensively melting snow under clear sky (Eq. 1). Our ancillary SL501 data on another smaller open field showed a decline of $A = -0.0028 \cdot \text{SZA}$ the same clear sky day. Although the decline for our SL501 and Bentham data are similar, the values of the spring time snow albedo gained from Bentham measurements on a big open field (albedo values around 0.45–0.72)

ACPD
10, 27075–27098, 2010

and SL501 on a smaller field (albedo around 0.37–0.51) differed from each other. This may be due to the differences in the wavelength range and the area under study, as well as differences in snow properties (grain size, water content etc.). On the basis of these albedo results, it would appear that for melting snow, the albedo decline could be in the Arctic and Antarctic of the same magnitude:

$$A = A_{\text{midday}} + c(\text{SZA} - \text{SZA}_{\text{min}}), \text{where } c = [-0.0030, -0.0024]. \quad (4)$$

Independently from this albedo decline due to melt of the snow, albedo of snow showed an increase as a function of wavelength. The increase in snow albedo (Fig. 3) is in accordance with theory, and Antarctic observations presented in Grennfell et al. (1994), e.g. On the other hand, Wuttke et al. (2006) found that in their Antarctic snow albedo data, the spectral dependence of the albedo in the UV and visible was not very pronounced. Feister and Grewe (1995), in turn, have performed spectral albedo measurements over bare fertile soil, sand at the beach, concrete and snow. They found that the albedo increases with increasing wavelengths for most types of surfaces considered, i.e., it was smaller in the UV than in the visible region. According to Feister and Grewe, the measured albedo over polluted snow was 0.62–0.76% in the UVB region ($\lambda < 315$ nm), with a small wavelength dependence. A somewhat higher albedo occurred in the UVA region ($315 < \lambda < 400$ nm). Thus, as a summary, it would appear that a spectrally dependent albedo signal is often behind the broadband albedo. To achieve as accurate albedo estimates as possible, the spectral behavior in snow albedo needs to be considered. Our simple empirical regression results on converting UVA, UVB, and VIS albedo from one to another may serve as a tool for any application where the albedo is measured at one wavelength range, but the interest lies on another (Eqs. 2 and 3). Earlier, Li and Trishchenko (1999) have made a study on the development and validation of narrow band to broadband conversion models. According to them, a linear regression (a basic conversion model) between shortwave (SW) albedo (α_{sw}) and VIS albedo (α_{vis}): $\alpha_{sw} = a_0 + b_0\alpha_{\text{vis}}$ that does not require any auxiliary information, has been most widely used. For snow and ice, they

ACPD
10, 27075–27098, 2010

give $a_0 = 10.802$ and $b_0 = 0.725$. Our basic conversion regression approach is similar to that, but between UV and VIS albedo. The next step would be to introduce SZA, and thereafter other environmental parameters, into the conversion model. To do that, a larger data set would be required. Here, the snow grain sizes of the melting Arctic snow represented the range from 0.25 mm to several millimeters, which values are larger compared to many other studies; e.g., 0.8 mm in Wuttke et al. (2006); and 1 mm in Warren and Wiscombe (1980) and Wiscombe and Warren (1980). It would appear that the grain sizes of the melting European Arctic snow might be bigger than those of Antarctic or Alpine snow.

A variety of climatological studies including radiative forcing of the planet are dependent on snow albedo assumptions at given seasons. For melting snow seasons these assumptions have to be very carefully implemented on various modeling codes. Our results suggest, that for the satellite retrieval of snow UV reflectance during melt time, the actual time of satellite observation has influence on the obtained albedo results: in the morning the albedo may be expected higher than later the day (according to the Eq. 4). Also, during snow melt, the effective surface UV albedo distributions; like presented in Tanskanen and Manninen (2007), and Robinson and Kukla (1984); are expected to move left along the x-axis (toward smaller values). We may expect that snow height dependent parameterizations (like in Arola et al., 2003), in turn, might function well during melt time. In the UCAR Atmospheric model (CAM 3.0), the melting snow parameterization depends linearly on surface temperature Ts according to $0.1 \cdot (Ts + 1)$ (Collins et al., 2004). The snow and ice albedo parameterization depending on temperature is in the ECHAM5 model (Roeckner et al., 2003; Roesch and Roeckner, 2006), too. In the ECWMF model, albedo parameterization is with temperature (exponential relationship) and snow fall occurrence (ECWMF, 2010). According to Pirazzini (2008), the representation of the snow and ice albedo for climate and numerical weather prediction models may be one of the most serious oversimplifications, and this may cause large errors in weather prediction and climate simulations. In the paper by Cheng et al. (2006) it has been shown, that in the case that the albedo parameterization is too

ACPD
10, 27075–27098, 2010

Title Page
Abstract Introduction
Conclusions References
Tables Figures
◀◀ ▶▶
◀ ▶
Back Close
Full Screen / Esc
Printer-friendly Version
Interactive Discussion

sensitive to surface temperature, errors in the surface energy and mass balance grow rapidly due to the strong positive feedback between albedo and temperature errors. According to Pedersen and Winther (2005), snow depth-dependent parameterizations perform better during the snowmelt period than temperature-dependent parameterizations. Furthermore, Pirazzini (2008) has presented a simulation experiment with the two-dimensional mesoscale HIRLAM model of the University of Helsinki, Finland, where the old snow albedo of 0.7 was used instead the measured albedo of 0.83 (fresh snow). According to their sensitivity runs, they concluded that in the case of fresh snow, the use of old snow albedo and thermodynamic values caused, alone, a delay in the surface cooling, and about 3 °C of error in the surface temperature. Therefore, we might expect that the differences in snow albedo during melt, with variation from 0.8 to 0.4 as shown in our results, might cause a significant effect, too.

We have been investigating the April snow melting period for the specific area of Northern Finland, and the spectral and temporal variations of snow albedo during this period. Using RT calculations, spectral and temporal information on the effect of albedo change on UV irradiances were gained. In our case, it was shown that melting snow can be the source of irradiance differences up to 9% if modeled results do not take into account the change of the albedo in the melting period. Our RT calculation results also showed that if we under- or overestimate the albedo, even with a realistic value, the difference in calculated irradiances are effected as a function of wavelength. Therefore, during snow melt, the snow albedo, used in various RT models, have to be carefully implemented and not assumed a priori.

Acknowledgements. The work has been supported by the Academy of Finland (SAARA-project).

References

Arola, A., Kaurola, J., Koskinen, L., Tanskanen, A., Tikkanen, T., Taalas, P., Herman, J. R., Krotkov, N., and Fioletov, V.: A new approach to estimating the albedo for

ACPD
10, 27075–27098, 2010

Spectral albedo of arctic snow during intensive melt period

O. Meinander et al.

snow-covered surfaces in the satellite UV method, J. Geophys. Res., 108, D17, 4531, doi:10.1029/2003JD003492, 2003.

Bernhard, G. and Seckmeyer, G.: Uncertainty of measurements of spectral solar UV irradiance, J. Geophys. Res., 104, D12, 14321–14345, 1999.

Bernhard, G., Booth, C. R., Ehramjian, J. C., Stone, R., and Dutton, E. G.: Ultraviolet and visible radiation at Barrow, Alaska: Climatology and influencing factors on the basis of version 2 National Science Foundation network data, J. Geophys. Res., 112, D09101, doi:10.1029/2006JD007865, 2007.

Cheng, B., Vihma, T., Pirazzini, R., and Granskog, M. A.: Modelling of superimposed ice formation during the spring snowmelt period in the Baltic Sea, Ann. Glaciol., 44, 139–146, 2006.

Christner, B. C., Morris, C. E., Foreman, C. M., Cai, R., and Sands, D. C.: Ubiquity of Biological Ice Nucleators in Snowfall, Science, 29 February 2008, 319, 5867, 1214, doi:10.1126/science.1149757, 2008.

Collins, W. D., Rasch, P. J., Boville, B. A., Hack, J. J., McCaa, J. R., Williamson, D. L., Kiehl, J., Briegleb, B., Bitz, C., Lin, S.-J., Zhang, M., and Dai, Y.: Description of the NCAR Community Atmosphere Model (CAM 3.0), NCAR/TN-464+STR NCAR TECHNICAL NOTE June 2004, http://www.cesm.ucar.edu/models/atm-cam/docs/description/node35.html, 2004.

ECWMF, The European Centre for Medium-Range Weather Forecasts, The ECMWF Integrated Forecast System (IFS), IFS documentation CY25r1, operational on 9 April 2002, Eq. 7.29 at http://www.ecmwf.int/research/ifsdocs/CY25r1/Physics/Physics-08-05.htm, 2010.

Feister, U. and Grewe, R.: Spectral Albedo Measurements in the UV and Visible Region Over Different Types of Surfaces, Photochem. Photobiol., 62, 4, 736–744, 1995.

Grannas, A. M., Jones, A. E., Dibb, J., Ammann, M., Anastasio, C., Beine, H. J., Bergin, M., Bottenheim, J., Boxe, C. S., Carver, G., Chen, G., Crawford, J. H., Dominé, F., Frey, M. M., Guzmán, M. I., Heard, D. E., Helmig, D., Hoffmann, M. R., Honrath, R. E., Huey, L. G., Hutterli, M., Jacobi, H. W., Klán, P., Lefer, B., McConnell, J., Plane, J., Sander, R., Savarino, J., Shepson, P. B., Simpson, W. R., Sodeau, J. R., von Glasow, R., Weller, R., Wolff, E. W., and Zhu, T.: An overview of snow photochemistry: evidence, mechanisms and impacts, Atmos. Chem. Phys., 7, 4329–4373, doi:10.5194/acp-7-4329-2007, 2007.

Grenfell, T. C., Warren, S. G., and Mullen, P. C.: Reflection of solar radiation by the Antarctic snow surface at ultraviolet, visible, and near-infrared wavelengths, J. Geophys. Res., 99, D9, 18669–18684, 1994.

Kylling, A., Persen, T., Mayer, B., and Svenøe, T.: Determination of an effective spectral surface

ACPD
10, 27075–27098, 2010

albedo from ground-based global and direct UV irradiance measurements, J. Geophys. Res., 105, D4, 4949–4959, 2000.
Li, Z. and Trishchenko A.: A Study toward an Improved Understanding of the Relationship between Visible and Shortwave Measurements, J. Atmos. Ocean. Tech., 16, 347–360, 1999.
Mayer, B. and Kylling, A.: Technical note: The libRadtran software package for radiative transfer calculations – description and examples of use, Atmos. Chem. Phys., 5, 1855–1877, doi:10.5194/acp-5-1855-2005, 2005.
Meinander, O., Kontu, A., Lakkala, K., Heikkilä, A., Ylianttila, L., and Toikka, M.: Diurnal variations in the UV albedo of arctic snow, Atmos. Chem. Phys., 8, 6551–6563, doi:10.5194/acp-8-6551-2008, 2008.
Meinander, O., Wuttke, S., Seckmeyer, G., Kazadzis, S., Lindfors, A., and Kyrö, E.: Solar zenith angle asymmetry cases in polar snow UV albedo, Geophysica, 45, 1–2, http://www.geophysica.fi/pdf/geophysica_2009_45_1-2_183_meinander.pdf, 2009.
Pedersen, C. A. and Winther, J.-G.: Intercomparison and validation of snow albedo parameterization schemes in climate models, Clim. Dynam., 25, 351–362, 2005.
Pirazzini, R.: Surface albedo measurements over Antarctic sites in summer, J. Geophys. Res., 109, D20118, doi:10.1029/2004JD004617, 2004.
Pirazzini, R.: Factors controlling the surface energy budget over snow and ice. PhD Thesis. 141 p. Finnish Meteorological Institute Contributions 73. https://oa.doria.fi/bitstream/handle/10024/42713/factorsc.pdf?sequence=1, 2008.
Pirazzini, R., Vihma, T., Granskog, M., and Cheng, B.: Surface albedo measurements over sea ice in the Baltic Sea during the spring snowmelt period, Ann. Glaciol., 44, 7–14, 2006.
Roeckner, E., Bäuml, G., Bonaventura, L., Brokopf, R., Esch, M., Giorgetta, M., Hagemann, S., Kirchner, I., Kornblueh, L., Manzini, E., Rhodin, A., U. Schlese, U., Schulzweida U., and Tompkins, A.: The atmospheric general circulation model ECHAM5 , Part I, Model description, Report 349, Max Planck Institute for Meteorology, ISSN 0937 – 1060, http://www.mpimet.mpg.de/fileadmin/models/echam/mpi_report_349.pdf, 2003.
Roesch, A. and Roeckner, E.: Assessment of Snow Cover and Surface Albedo in the ECHAM5 General Circulation Model, J. Climate, 19, 3828–3843, 2006
Robinson, D. A. and Kukla, G.: Maximum surface albedo of seasonally snow-covered lands in the Northern Hemisphere, J. Clim. Appl. Meteorol., 24, 402–411, 1984.
Roujean, J.-L., Manninen, T., Kontu, A., Peltoniemi, J., Hautecoeur, O., Riihelä, A., Lahtinen, P., Siljamo, N., Suokanerva, H., Sukuvaara, T., Kaasalainen, S., Aulamo, O., Aaltonen, V.,

ACPD
10, 27075–27098, 2010

Thölix, L., Karhu, J., Suomalainen, J., Hakala, T., and Kaartinen, H.: "SNORTEX (Snow Reflectance Transition Experiment): Remote sensing measurement of the dynamic properties of the boreal snow-forest in support to climate and weather forecast: report of IOP-2008." 2009 IEEE International Geosci. Remote Sensi. Symposium, 12–17 July, Cape Town, South Africa (Paper 1167), 2009.

Roujean, J.–L., Manninen, T., Sukuvaara, T., Peltoniemi, J., Kaasalainen, S., Hautecoeur, O., Lahtinen, P., Riihelä, A., Siljamo, N., Lötjönen, M., Karjalainen, T., Kontu, A., Suokanerva, H., Aulamo, O., Lemmetyinen, J., Suomalainen, J., Hakala, T., Kaartinen, H., Thölix, L., Meinander, O., and Karhu, J.: SNORTEX: Remote sensing measurement of snowmelt in European boreal forest, iLEAPS Newsletter Issue No. 9, April 2010, http://www.ileaps.org/index.php?option=com_phocadownload\&view=category\&id=3:\&Itemid=81, 2010.

Seckmeyer, G., Bais, A., Bernhard, G., Blumthaler, M., Booth, C. R., Lantz, K., and McKenzie, R. L.: Instruments to measure solar ultraviolet radiation, part 2: Broadband instruments measuring erythemally weighted solar irradiance, WMO GAW Report, 2005.

Schwander, H., Mayer, B., Ruggaber, A., Albold, A., Seckmeyer G., and Koepke, P.: Method to determine snow albedo values in the UV for radiative transfer modelling, Appl. Optics, 38, 18, 3869–3875, 1999.

Tanskanen, A. and Manninen, T.: Effective UV surface albedo of seasonally snow-covered lands, Atmos. Chem. Phys., 7, 2759–2764, doi:10.5194/acp-7-2759-2007, 2007.

Warren, S. G. and Wiscombe, W. J.: A model for the spectral albedo of snow. II: Snow containing atmospheric aerosols, J. Atmos. Sci., 37, 2734–2745, 1980.

Wiscombe, W. J. and Warren, S. G.: A model for the spectral albedo of snow. I: Pure snow, J. Atmos. Sci., 37, 2712–2733, 1980.

WMO Guide to Meteorological Instruments and methods of Observation, WMO-No. 8 (Seventh Edition, 6 August 2008), http://www.wmo.int/pages/prog/www/IMOP/publications/CIMO-Guide/CIMO_Guide-7th_Edition-2008.html, 2008.

Wuttke, S., Seckmeyer, G., and König-Langlo, G.: Measurements of spectral snow albedo at Neumayer, Antarctica, Ann. Geophys., 24, 7–21, doi:10.5194/angeo-24-7-2006, 2006.

Zhou, X., Li, S., and Stamnes, K.: Effects of vertical inhomogeneity on snow spectral albedo and its implication for optical remote sensing of snow, J. Geophys. Res., 108, D23, ACL11.1-ACL11.15, 2003.

Table 1. Snow conditions during the time [UTC] of the spectral albedo measurements.

Day/Time	Snow Surface
20 April	
17:46	Snowball test: no
21 April	
13:50	Snowball test: no, grain size 0.25 mm, a new snow layer, icy snow
16:38	Snowball test: yes, 1 mm grains melted together, sunny cloudless calm weather; melting snow, new snow layer exists
17:30	Wet new snow layer exists, surface layer of 0.5 cm
18:19	Snowball test: no
22 April	
12:35	No new snow layer, icy snow, 0.5 cm surface layer with grains minimum 0.25 mm, maximum 1 mm, all stick together; the rest of the snow is 1.5–5 mm grains and sticks together
13:00	1 mm grains, sunny weather, clear sky
13:58	2 mm grains on the surface
15:17	Snowball test: yes, 2–3 mm grains on the surface, wet snow
16:08	3 mm grains
17:12	Snowball test: yes, 3 mm grains, wet snow
20:17	Wet snow, 3 mm grains, fluffy surface

ACPD
10, 27075–27098, 2010

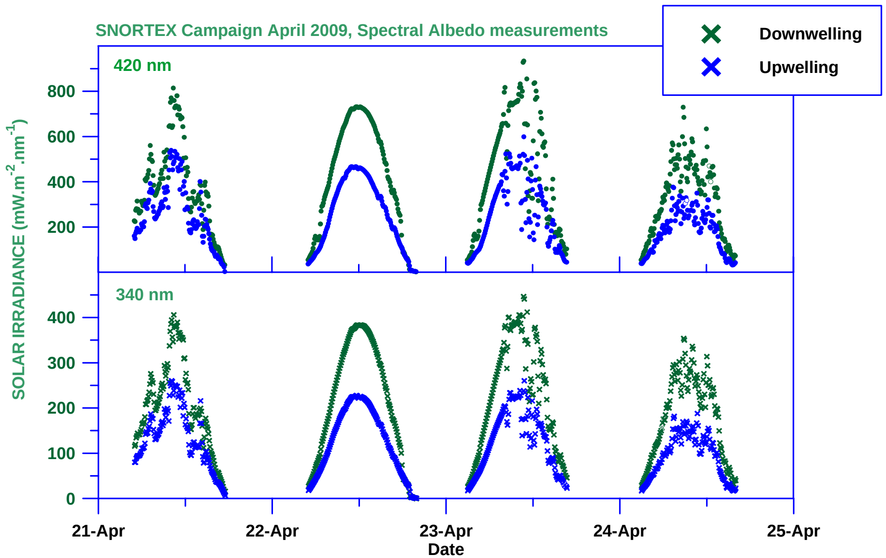

Fig. 1. Global downwelling and upwelling irradiance for 340 nm and 440 nm during the campaign.

ACPD
10, 27075–27098, 2010

Spectral albedo of arctic snow during intensive melt period

O. Meinander et al.

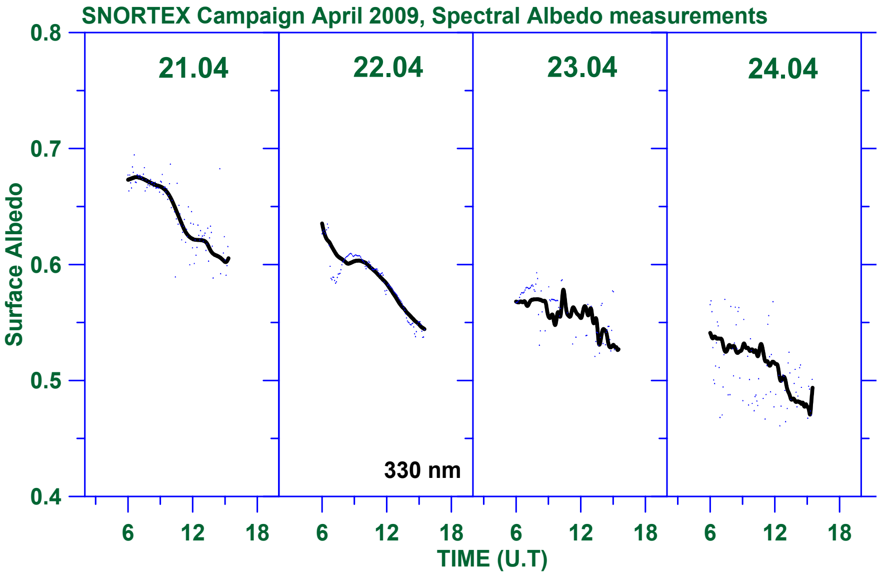

Fig. 2. Snow albedo at 330 nm, during 21 – 24 April, 2009. Blue dots represent 6 min period measurements, and black line time interpolated 1 min ratios.

ACPD
10, 27075–27098, 2010

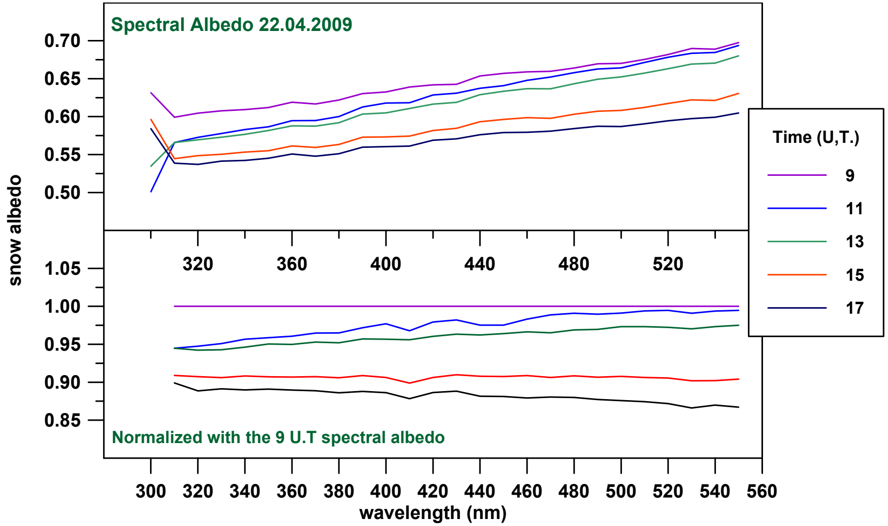

Fig. 3. The snow albedo increased as a function wavelength. (Up) Spectral snow albedo for 22 April for different periods during the day. (Down) Ratio of each of the above spectral measurements with the 09:00 UTC measurement.

ACPD
10, 27075–27098, 2010

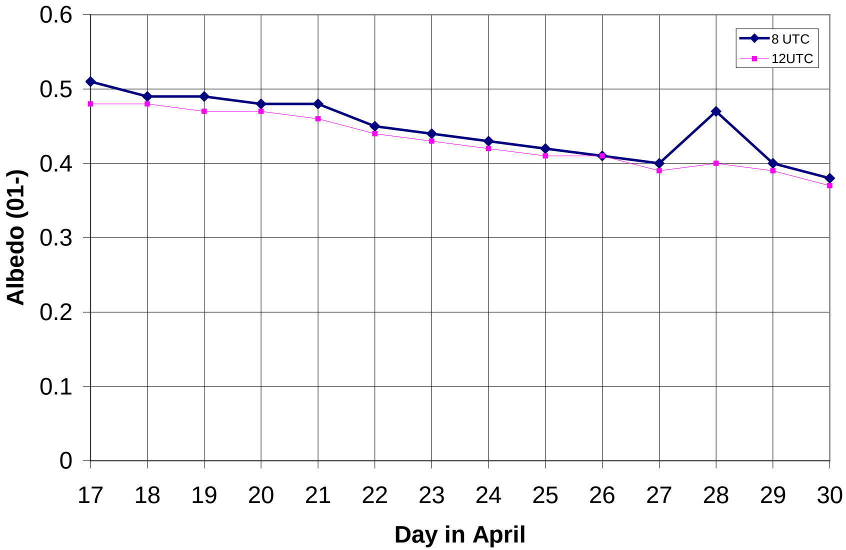

Fig. 4. The erythemal UV albedo of snow from 17 April to 30 April, 2009. The albedo decline during day: blue line for 08:00 UTC, purple line for 12:00 UTC.

ACPD
10, 27075–27098, 2010

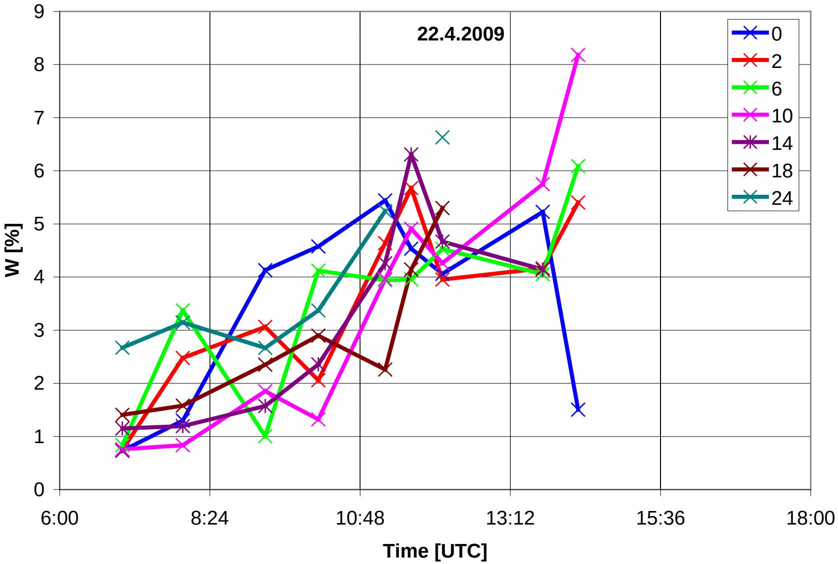

Fig. 5. The snow water liquid content, as a function of time and snow depth (0, 2, 6, 10, 14, 18, 24 cm) on 22 April. The data shows that the water content first increased in the surface layer, and after several hours of accumulation moved into deeper layers.

ACPD
10, 27075–27098, 2010

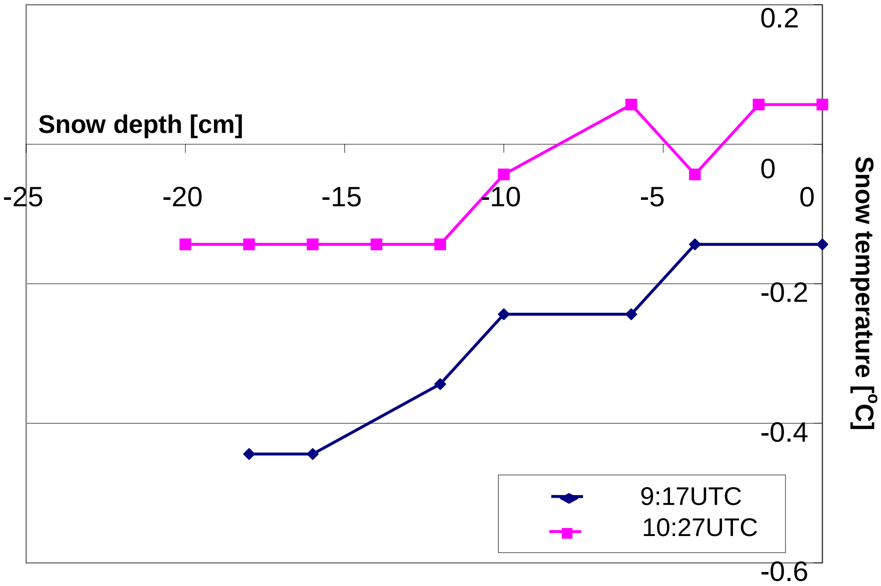

Fig. 6. The snow temperature (y-axis) profile showed both vertical and temporal increase during the study days. Blue line marks for temperature measured at 09:17 UTC 22 April, and magenta for appr. one hour later, 10:27 UTC, at depths from 20 cm to the snow surface layer (0 cm). Despite the calibration of the temperature measurement, some results are above zero. This may be due to, e.g., the mixture of snow-air-water that is measured in the case of melting snow.

ACPD
10, 27075–27098, 2010

Spectral albedo of arctic snow during intensive melt period

O. Meinander et al.

Title Page
Abstract | Introduction
Conclusions | References
Tables | Figures
◀| |▶
◀ ▶
Back | Close
Full Screen / Esc
Printer-friendly Version
Interactive Discussion

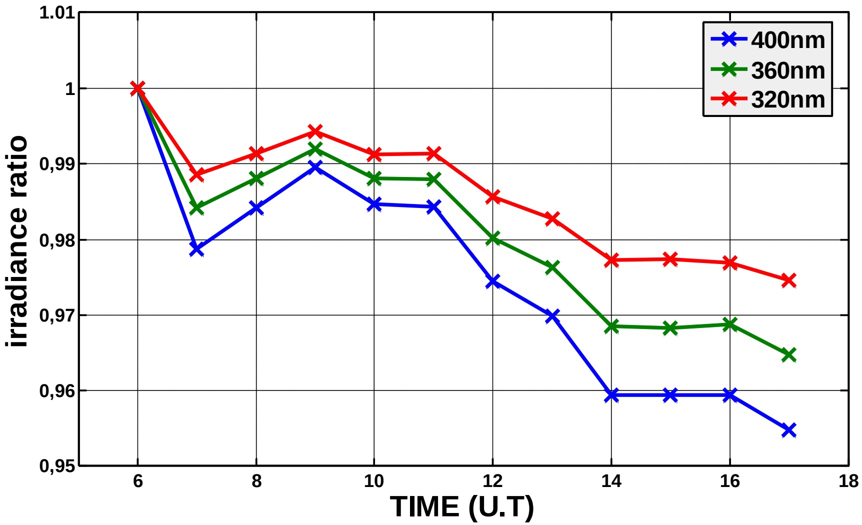

Fig. 7. The ratios of modeled irradiances using maximum measured albedo A_{max} for 22 April, and measured albedo A for the same day.

ACPD
10, 27075–27098, 2010